Scanning Microscopy

Volume 10 | Number 1 Article 8

11-17-1995

Quantitative Imaging in Electron and Confocal Microscopies for Applications in Biology

N. Bonnet
University of Reims, noel.bonnet@univ-reims.fr

L. Lucas
University of Reims

D. Ploton
University of Reims

Scanning Microscopy Vol. 10, No. 1, 1996 (pages 85-102) 0892-953X/96$5.00+.25
Scanning Microscopy International, Chicago (AMF O'Hare), IL 60666 USA

QUANTITATIVE IMAGING IN ELECTRON AND CONFOCAL MICROSCOPIES FOR APPLICATIONS IN BIOLOGY

N. Bonnet*, L. Lucas and D. Ploton

INSERM Unit 314, University of Reims, 21, rue Clément Ader, 51685 Reims Cedex 2, France

(Received for publication May 11, 1995 and in revised form November 17, 1995)

Abstract

Among the large number of topics related to the quantification of images in electron and confocal microscopies for applications in biology, we selected four subjects that we consider to be representative of some recent tendencies. The first is the quantification of three-dimensional data sets recorded routinely in scanning confocal microscopy. The second is the quantification of the textural and fractal appearance of images. The two other topics are related to image series, which are more and more often provided by imaging instruments. The first kind of series concerns electron energy-filtered images. We show that the parametric (modelling) approach can be complemented by non-parametric approaches (e.g., different variants of multivariate statistical techniques). The other kind of series consists of multiple mappings of a specimen. We describe several new tools for the study and quantification of the co-location, with potential application to multiple mappings in microanalysis or in fluorescence microscopy.

Key Words: Image processing, quantification, electron microscopy, confocal microscopy, microanalysis.

*Contact for correspondence:
N. Bonnet, address as above.
Telephone number: 33-2605-0752
FAX number: 33-2605-1900
E-mail: noel.bonnet@univ-reims.fr

Introduction

Many imaging instruments are now available on the market for producing images of biological structures. These instruments cover a large range of resolution, from the sub-millimeter range obtained with optical microscopes operating at low magnification to the nanometer range which can be reached by near-field microscopes (tunnel and atomic force microscopes). Between these two extremes of the scale, the confocal microscope and the different kinds of electron microscopes, transmission (TEM), scanning (SEM) and scanning transmission (STEM) fill the gap. Each of these microscopes, and others like the X-ray microscope, the Raman microscope and the acoustic microscope, for instance, have their own constraints and peculiarities, which make it impossible to observe the same specimen with the different microscopes. It is, however, possible to record images at different scales.

The scale is not the only parameter that distinguishes the various kinds of images available. The nature of these images and the different types of information they provide can also be different. This information can be of a topographic, "functional" or chemical nature. Near-field microscopes, for instance, provide information mainly related to the surface topography, and it is relatively difficult to infer information about the interior of the objects. This is also approximately true for SEM. Conventional optical microscopy and TEM give information related to the relative density of the observed structures. Fortunately, staining techniques allow us to selectively increase the density of a large number of constituents, which can thus be observed with higher contrast than in their natural state. When this kind of feature selection is inoperative, other approaches can be used to highlight specific features. These approaches include: cytochemistry, immunocytochemistry, fluorescence microscopy and *in situ* hybridization. These operative modes make it possible to obtain "functional" images of the specimen, where the main interest is not only in the topography of the substructures but also in the number of features present (antigenic sites, fluores-

cent sites, etc.), revealed by the pre-imaging procedure.

Besides these imaging methods, there is also a panoply of methods designed to reveal the chemical nature of the constituents of a specimen. These methods constitute the microanalytical adjuncts to microscopy which can be performed with optical (fluorescence, Raman, infra-red microanalysis), electron (X-ray, electron energy-loss, Auger microanalysis) or ion microscopes. At first, the microanalytical techniques were either of spectroscopic or imaging nature. But recently, these two kinds of activities have become completely integrated, and the emergence of spectrum-imaging techniques is one of the most promising tendencies of the microscopic science.

All these kinds of images and related information (morphometric, functional or microanalytical) need to be quantified if one wants to get the best out of the efforts made to develop such sophisticated instruments.

The quantification of the information contained in images of biological specimens is not in its infancy, and reviewing all the approaches followed during the last thirty years is beyond the scope of this article {additional subjects are treated in the textbooks (Castelman, 1979; Hawkes, 1980; Russ, 1990a)}. Instead, we have made a selection of a few topics which illustrate some tendencies of quantification for two of the three categories of images mentioned above.

For the morphometric information, we have selected two topics. The first concerns the tendency to extrapolate from image analysis in two-dimensions (2D) to three-dimensional (3D) image analysis. This tendency is particularly evident within the framework of confocal microscopy, where it is so easy to produce three-dimensional data sets that measurement in two dimensions only is no longer justified. The tendency is less clear in electron microscopy because three-dimensional microtomography is not yet a routine technique, despite encouraging recent developments. The 3D pre-processing, reconstruction and quantification of confocal images is described in the next section.

As a second topic in this category, we have selected the quantification of textural and fractal characteristics of images.

For the third kind of information, i.e., information related to the chemical composition of a specimen, we have also selected two topics. The first concerns the processing of electron energy-filtered image series, which can be recorded with a TEM or a STEM equipped with a spectrometer in order to characterize the content of a specimen by studying the energy lost by the electrons. Several data processing techniques are in competition for the extraction of the useful information from such image sequences. Since these sequences are the precursors of what is now being generalized as spectrum-images in different microscopical techniques, it seems interesting to discuss the different strategies.

Finally, we will discuss the case of multiple mapping. With several microanalytical techniques, such as energy-dispersive X-ray analysis (EDX), electron energy loss spectroscopy (EELS), secondary ion mass spectroscopy (SIMS), we are able to record several maps related to the concentration of various constituents within the specimen. The next problem is thus to find ways of deducing a synthetic map of regions with homogeneous composition in order to perform a subsequent quantification in terms of the number of such regions, areas of the different regions, spatial distribution, etc. Some tools for answering these kinds of questions will be described.

Quantification of Morphometry in Three-Dimensional Confocal Microscopy

The principle of the confocal microscope is now well known (readers are referred to the textbooks, e.g., Pawley, 1990): due to the confocality principle, the depth of field is reduced to less than 0.5 μm so that optical sections of the specimen can be obtained. By stepping the focus plane and recording a set of serial sections, it is possible to reconstruct the three-dimensional object in the computer. Since different fluorochromes can label different antibodies and several laser illuminations and several photomultipliers can be used, multiple three-dimensional maps of the object under study can in principle be recorded. Other operating modes (reflection mode for instance) can also provide additional information.

This offers exciting perspectives for the extraction of quantitative 3D information from biological specimens.

Below, we describe some developments we have made in this direction, along with a brief review of the work done by others.

One of the requirements of 3D quantitation compared to 2D quantitation is that 3D reconstruction must be performed as a preliminary step. Despite many recent improvements, 3D reconstruction in microscopy is still a difficult task, especially when quantitative results are to be extracted in addition to qualitative information (Turner, 1981). In electron microscopy (microtomography), the main difficulty is to cope with the limited solid angle available with goniometer stages (Frank, 1992). In optical and confocal microscopy, the principle of 3D reconstruction is very simple: it consists of stacking optical serial sections into the reconstructed digital volume. However, although a crude improvement can be obtained with confocal microscopes, both instruments are still characterized by an anisotropic impulse response which results in an elongation of objects along the "z" direction. This distortion must be corrected when quan-

titative information is to be obtained. Many methods are now available for performing this task, which is called deblurring (because the imaging process consists of a blur of each plane by the adjacent planes) or deconvolution (because the 3D imaged volume is the convolution of the original object against the impulse response of the imaging instrument) (Agard *et al.*, 1989; Katsaggelos, 1991). These methods include:

[1] The nearest neighbor method (Castelman, 1979):

$$\hat{O}_i = I_i - [I_{i+1} * h_1 + I_{i-1} * h_{-1}] * k_1 \qquad (1)$$

where $\hat{O}_i$ is the estimation of the intensity of the i^{th} object plane, I_i is the intensity of the i^{th} image plane, h_1 and h_{-1} are low-pass (blurring) filter kernels describing the influence of the neighbor object planes O_{i-1} and O_{i+1} on the current image plane I_i, k_1 is a high-pass (deblurring) kernel and * is the convolution operator.
{Note that attempts to avoid using neighbor planes for performing image restoration (Monck *et al.*, 1992) cannot be considered as belonging to the class of 3D restoration methods, despite the claim of the authors}.

[2] The Wiener filter method (Holmes *et al.*, 1991):

$$\hat{O} = FT^{-1}[\ \ddot{O}\ ] \qquad (2)$$

where $\hat{O}$ is the estimation of the restored object, $\ddot{O}$ the estimation of its frequency spectrum, and FT^{-1} is the inverse Fourier transform:

$$\ddot{O} = \ddot{I} \cdot \frac{H^*}{|H|^2 + |N/S|^2} \qquad (3)$$

where $\ddot{I}$ is the frequency spectrum of the imaged volume, H is the imaging transfer function (the Fourier Transform of the 3D impulse response), and $|N/S|^2$ is the inverse of the signal-to-noise ratio (expressed in the frequency domain).

The drawback of this method is that, since the signal-to-noise frequency spectrum cannot be known precisely, there is a risk of amplifying noise in the restored object, especially at frequencies where H is very small.

[3] The Jansson-van Cittert procedure (Jansson *et al.*, 1970): this is an extension of the nearest-neighbor approach where estimates of the object function $\hat{O}_{(k)}$ are iteratively improved until it becomes compatible with the experimental image I and the 3D impulse response h:

$$\hat{O}_{(k+1)} = \text{Max}\ \{0,\ \hat{O}_{(k)} + \gamma \cdot [I - \hat{O}_{(k)} * h]\} \qquad (4)$$

where γ is a gain factor, h is the 3D low-pass (blurring) kernel, and k is the iteration number. It has been shown (Kawata and Ichioka, 1980) that when the associated transfer function H is not positive for all frequencies, this procedure cannot converge and that, in that case, a

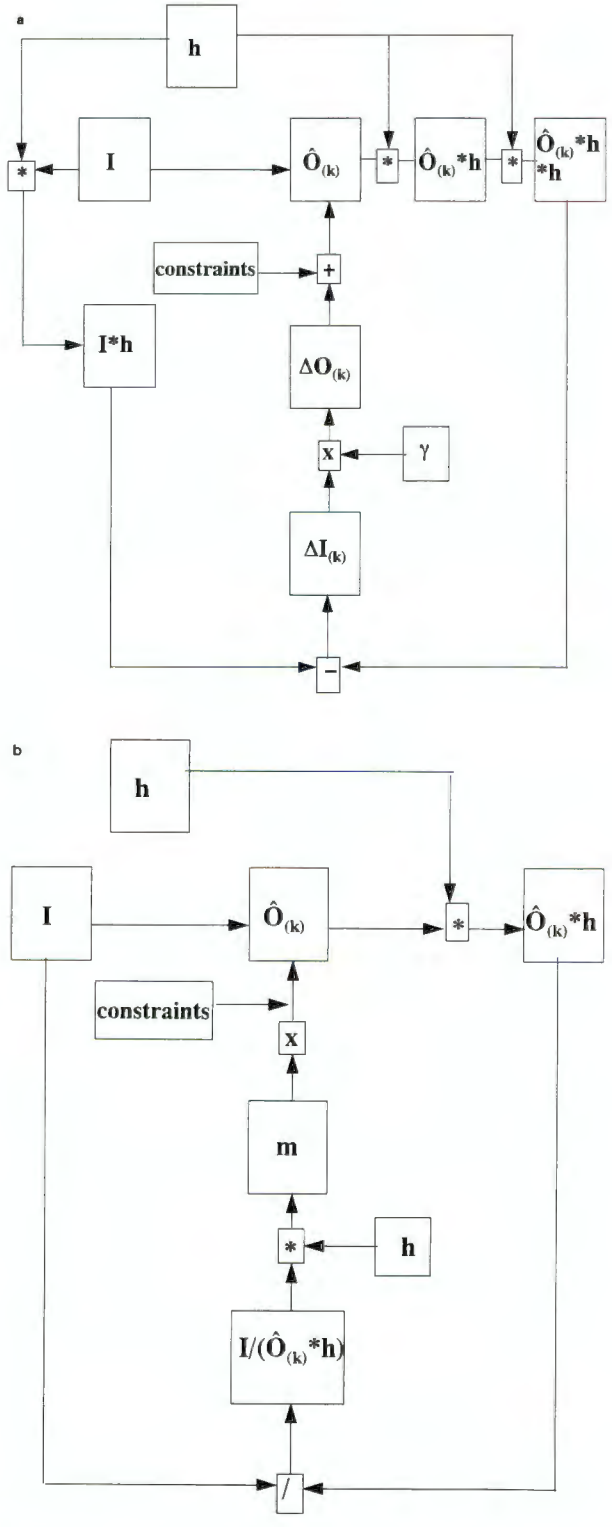

Figure 1. Schematic diagrams illustrating two iterative approaches for the restoration of images degraded by a three-dimensional blurring kernel. **(a)** The Jansson-van Cittert procedure, with the reblurring variant. **(b)** The maximum likelihood approach (so-called Richardson/ Lucy approach). The notations are those of the text.

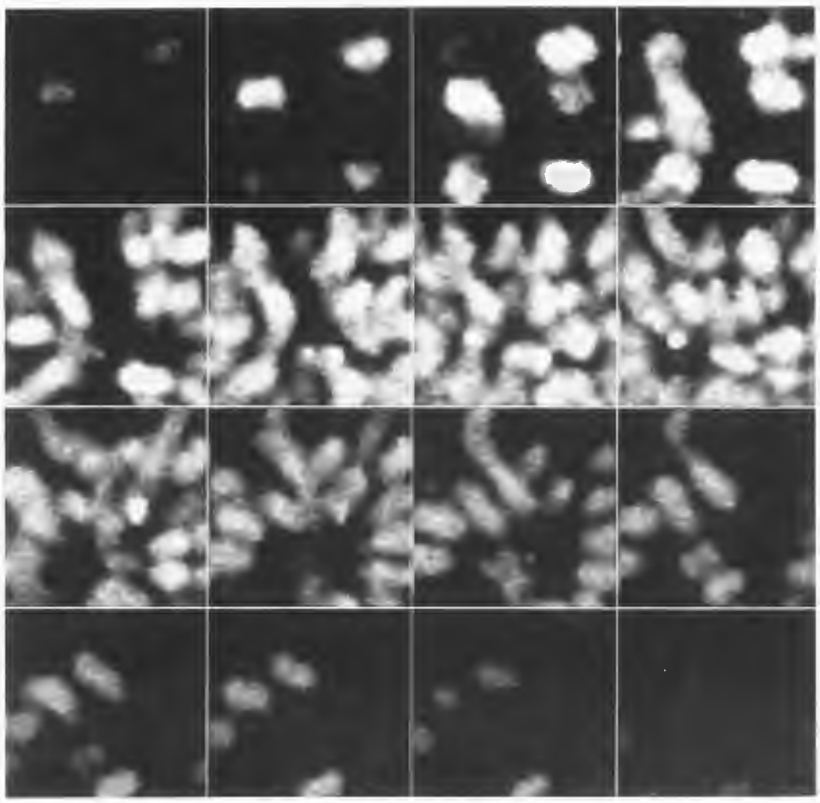

Figure 2. Gallery of the central parts of 16 serial sections of a cancerous cell in metaphasic state, stained with chromomycin A3, recorded with a confocal microscope. This data set is used for three-dimensional (3D) reconstruction, 3D restoration and 3D quantitation.

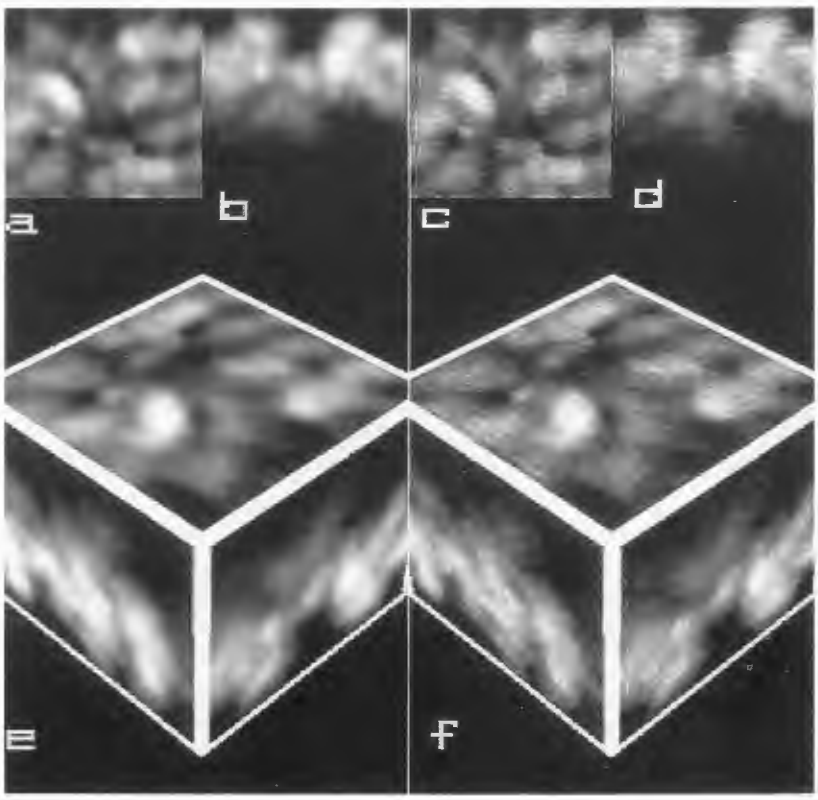

Figure 3. Visualisation of the central part of the 3D digital volume before (**a, b and e**) and after (**c, d and f**) 3D deblurring. The projection mode used was the integration mode. (**a and c**) Projections of the data set onto the horizontal X-Y plane; (**b and d**) projections of the data set onto the vertical X-Z plane; and (**e and f**) simultaneous projection onto the three faces of the parallelepiped.

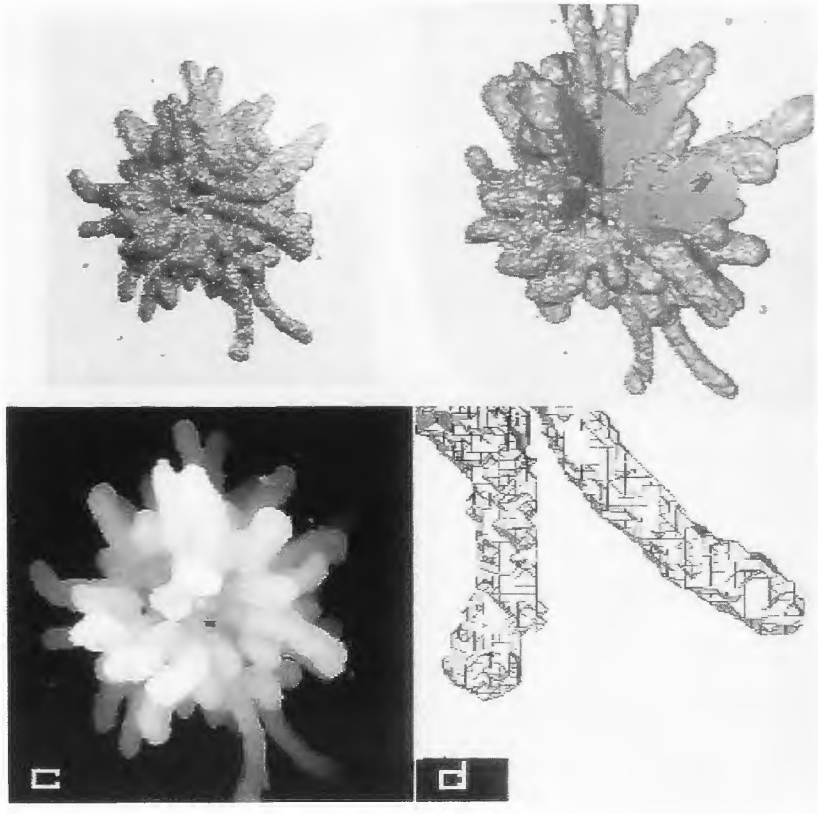

Figure 4. Some additional views of the reconstructed and restored digital volume. (**a**) Ray-tracing visualization mode. (**b**) Ray-tracing mode. The window allows visualization of the interior of the object and a check of its compactness. (**c**) Depth coding mode: the brighter parts are closer to the visualization point than the darker parts. (**d**) Magnified view of small parts of two chromosomes showing how the information is coded in the marching cube surface rendering module. Other visualization modes, such as, stereo-movies are also available.

reblurring procedure gives better results:

$$\hat{O}_{(k+1)} = \text{Max}\ \{0,\ \hat{O}_{(k)} + \gamma \cdot h * [I - \hat{O}_{(k)} * h]\} \quad (5)$$

The drawback of this approach is that it must be stopped before convergence because it converges towards the Wiener filter, with its associated deficiencies.

[4] The maximum likelihood (ML) approach: after its success in astronomy (Richardson, 1972; Lucy, 1974), the ML approach was introduced in confocal microscopy (Holmes and Liu, 1989; Willis *et al.*, 1993). It is also an iterative method which consists in refining the previous estimate of the object function according to the procedure:

$$\hat{O}_{(k+1)} = \text{Max}\ \{0,\ \hat{O}_{(k)} \cdot [I/(\hat{O}_{(k)} * h) * h]\} \quad (6)$$

This procedure can be iterated a large number of times without creating the artefacts produced by the Jansson-van Cittert or reblurring procedures.

The Jansson-van Cittert and maximum-likelihood procedures {eqs. (5) and (6), respectively} are represented by schematic diagrams in Figure 1.

Like several others, we have implemented all these methods (except the 3D Wiener filter) and have concluded that the ML approach gives the most satisfactory results, but at the expense of such a high computational load that it cannot be used routinely. Thus, we have developed a computational approach (based on the separation of a N-dimensional convolution kernel into N one-dimensional kernels) which reduces the computation time by a factor greater than ten (Bonnet, 1995c).

The restoration procedure is illustrated in Figures 2 and 3. Figure 2 is a gallery displaying 16 (out of 114) images of optical sections through a cancerous KB cell stained with chromomycin A3 in order to selectively visualize DNA in mitotic chromosomes {for more details concerning the specimen and the experimental protocol, see Ploton *et al.* (1994) and Gilbert *et al.* (1995)}. Figures 3a and 3b display horizontal ("x-y") and vertical ("x-z") projections of the reconstituted volume after interpolation and correction of the refractive index effect (Visser *et al.*, 1992). Figures 3c and 3d display the same projections after 3D image restoration (the microscope impulse response was determined experimentally by imaging fluorescent beads of size approximately equal to the voxel size). Figures 3e and 3f give an overview of the 3D data sets before and after restoration, respectively, through projections onto the three faces of the parallelepiped. Figure 4 shows some other views of the restored digital volume. The visualization modules were developed by us (Lucas, 1995; Lucas *et al.*, 1996a) and include: surface rendering {modified version of the marching cube algorithm (Lorensen and Cline, 1987)}, volume rendering and hybrid rendering

(ray-tracing, projection onto the parallelepiped faces). Movies can also be produced (Lucas *et al.*, 1996b).

Once volume reconstruction, volume restoration and volume display are complete, we can embark on the 3D quantification. As for image quantification, the most difficult task is the preliminary step which consists in isolating individual "objects," i.e., performing the segmentation of the 3D scene. Although specific staining procedures are generally used, the digitized volume is not often binary, and the full range of grey levels is often covered. Thus, advanced processing techniques developed for 2D images have to be extended to work on 3D data sets. They include: local pre-processing techniques for improving the signal-to-noise ratio and the contrast (Bonnet *et al.*, 1992a; Vautrot and Bonnet, 1994), mathematical morphology tools (Jeulin, 1988; Preston, 1991; Gratin and Meyer, 1992; Meyer, 1992), segmentation by the Voronoi diagram approach (Bertin *et al.*, 1992, 1993).

As an example of the difficulty of performing the segmentation task, we display in Figure 5a the histogram of the reconstructed and restored volume discussed previously (metaphase chromosomes). This histogram shows that the digital volume is far from being bimodal and that finding a grey level threshold for splitting the volume into "DNA" and "non-DNA" is not an easy task. We found that things become easier after local contrast enhancement. Among the different methods available, we used an extension of the local edge-based method (Beghdadi and Le Negrate, 1989). The histogram of the volume after contrast enhancement is shown in Figure 5b, and we can see that, although not yet binary, this histogram is to some extent bimodal. Thus, automatic methods (based on the Fisher criterion, or on entropy concepts) can be used to find the appropriate grey level threshold. Due to the overlapping of the two populations (stained/unstained), the binary image after thresholding is not perfect but after cleaning it (tools from mathematical morphology, such as closing/opening or relaxation procedures, can be used for this purpose), satisfactory results can be obtained.

Once individual objects, or regions, have been depicted and labelled, it is not a very difficult task to perform quantification. Parameters which can be quantified include: (1) the number of objects; (2) their surface and their volume; (3) some form factors, which can be deduced from their geometrical moments, for instance (Prokop and Reeves, 1992):

$$M_{pqr} = \Sigma\, i^p j^q k^r\, O(i,j,k)$$

$$\text{or } \mu_{pqr} = \Sigma\, (i-i_G)^p\, (j-j_G)^q\, (k-k_G)^r\, O(i,j,k) \qquad (7)$$

where O is the binary object function, i, j, k are spatial coordinates of voxels, and i_G, j_G, k_G are those of the center of mass G; and (4) their spatial distribution.

Some reports concerning 3D quantification in confocal microscopy can be found in König *et al.* (1991), Rigaut *et al.* (1991), Kett *et al.* (1992), Höfers *et al.* (1993), Usson *et al.* (1994) and Parazza *et al.* (1995).

We have implemented tools for performing such quantification studies. For instance, following Guilak (1994), we have found that the marching cube approach, which is one of the methods we have developed for 3D surface visualization, allows a fast and precise determination of surface and volume.

We are currently applying this software to the study of the quantitative modifications during the cell cycle of nucleolar proteins involved in the ribosomal transcription {RNA polymerase I and Upstream Binding Factor (UBF)} or involved in cell proliferation (KI-67 antigen).

Quantification of the Texture and Fractal Appearance

Biological structures often have a specific appearance that skilful observers are able to recognize as being different from one specimen to another one. However, grading and rating this difference in appearance is somewhat difficult and sometimes subjective. There is thus also a need to quantify these phenomena in addition to quantifying morphometric parameters (e.g., numbers, lengths, areas, or volumes).

Some of these problems are often referred to as texture recognition. This is the case of the texture of DNA in the nucleus for instance, which was long ago recognized as an important criterion for the characterization of cells in a normal or pathological state.

Others problems are referred to as fractal recognition. After the discovery of the fractal geometry by Mandelbrot (1982), it was realized that many biological structures have a fractal appearance, either by their external shape or by the grey level variations of their interior.

In this section, we give a brief survey and illustration of some recent approaches for characterizing image texture and fractalness.

Texture

As early as 1974, it was recognized that "stochastic characterization of texture should be generally useful for automatic recognition of cells by computer" and that "it is appropriate to examine quantitative descriptions of the texture of the cell nucleus" (Lipkin and Lipkin, 1974). In their study, a preliminary set of texture parameters was introduced to quantify the "fineness" or "coarseness" of the nucleus. After that, many studies were devoted to the definition of pertinent parameters for characterizing the chromatin texture at the optical microscope level (Pressman, 1976; Landeweerd and Gelsema,

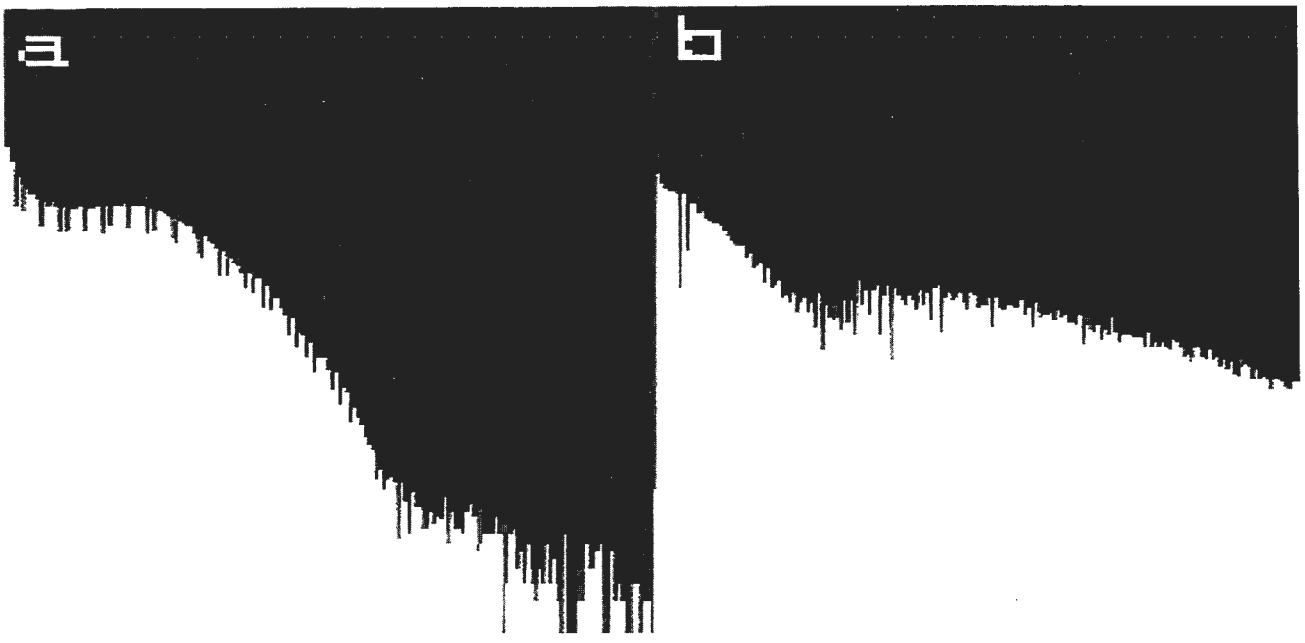

Figure 5. (a) Grey-level histogram of the restored digital volume (logarithmic scale). From this histogram, it is impossible to define a grey-level threshold for segmenting the volume into DNA/ non-DNA regions. (b) Grey-level histogram after local contrast enhancement. Though the bimodality is still imperfect, it is nevertheless possible to define a threshold for segmentation.

1978; Smeulders *et al.*, 1979; Komitowski and Zinser, 1985; Young *et al.*, 1986). Despite some variations, most of the approaches rely on methods based on estimations of the second-order statistics: the co-occurrence matrix and its secondary descriptors (Haralick, 1979) and the grey-level run length (Galloway, 1975). These features are also those which are used in most of the commercial software packages (Brugal, 1984).

Texture characterization is, of course, not limited to optical microscopy. Electron microscopes as well as confocal microscopes produce images in which texture play an important role and can be studied in great detail.

Figures 6a and 6b display images of chromatin texture recorded with a MRC 600 (BIORAD, Hemel, Hempstead, UK) confocal microscope (fluorochrome: chromomycin A3) {see Gilbert *et al.* (1995) for details of the experimental protocols}. The textural appearance in this kind of images is very dependent on the activity of the cell (quiescent or proliferating) and on the phase within the cell cycle (interphase or steps of mitosis).

Since the beginning of texture analysis, numerous tools have been explored for a better characterization of homogeneous or locally varying textures. Among these tools are: (1) Markov auto-regressive models (Pratt *et al.*, 1981), (2) filter banks (Unser and Eden, 1989), (3) Gabor filters (Jain and Farrhoknia, 1991), (4) wavelets (Vautrot and Bonnet, 1995; Unser, personal communication).

With these low-level tools, textural pattern recognition can be performed on a global basis (classification of different patterns into several classes) or on a local basis (segmentation).

Fractals

Many objects and structures (cells, organelles, tissues) display irregular patterns, which seem to have in common some self-similarity property (i.e., they have a similar appearance when they are observed at different magnifications). If this is so (or partly so), they can be described by the concepts of fractal geometry and especially by their fractal dimension.

This approach has been found useful in several fields of application: (1) image segmentation of lung sections (Rigaut, 1988), (2) characterization of cell surface complexity (Keough *et al.*, 1991; Nonnenmacher, 1994; Nonnenmacher *et al.*, 1994), (3) classification of retinal neurons according to their complexity (Fernandez *et al*, 1994), and (4) characterization of the microdistribution of elements in bioactive marine sediments (Block *et al.*, 1991).

A review of some methods, and other applications concerning the trabecular bone, exfoliative cervical cytology, neurons and glial cells, microbial growth patterns, marine organisms, mosaic organs and lung alveoli, can be found in Cross (1994).

There are now many ways of computing parameters connected to the self-similarity of curves and two-dimensional images:

[1] the box-counting approach (Gangepain and Roques-Carmes, 1986) and its variants (box-counting with interpolation (Keller *et al.*, 1989), differential box-counting (Chaudhuri *et al.*, 1993) and relative differential box counting (Jin *et al.*, 1995). Images are represented as pseudo-3D entities (the third dimension is given by the grey-level). The fractal dimension is estimated by D = -s, where s is the slope of the Log(N) - Log(L) curve. N is the number of cubic boxes (of size L) necessary to cover the whole 3D entity.

[2] the Hurst coefficient approach (Russ, 1990b): the local fractal dimension is given by D = 3 - s, where s is the slope of the Log(σ) - Log(d) curve, and σ is the standard deviation of grey levels of pixels situated a distance d away from a reference pixel.

[3] the power spectrum approach (Pentland, 1984; Aguilar *et al.*, 1993; Anguiano *et al.*, 1993): the power spectrum $P(f) = [I(f)]^2$, where I(f) is the Fourier Transform of the image, is computed and averaged along concentric rings (radius r). The slope s of the Log($P^{1/2}$) - Log(r) curve is related to the fractal dimension D by the relation: D = 4 - s.

[4] the mathematical morphology approach, also called the cover approach or the blanket approach (Peleg *et al.*, 1984; Maragos and Schafer, 1990; Maragos, 1994): the fractal dimension is estimated as D = 2 - s, where s is the slope of the curve Log(A) - Log(r). A is the area of the pseudo-3D entity (cf. the box-counting method) obtained after dilation of the original 3D entity by a structuring element of size r.

We have undertaken a comparative study of the conditions of application of these different methods (Bonnet *et al.*, 1994). Here, we can only give a brief illustration of some of the methods.

Images of chromatin similar to those discussed in the previous section are chosen as examples. Figures 6a and 6b represent two projected views of nuclear chromatin at slightly different states of interphase. We can discriminate the two slightly different textures. Figures 6c and 6d show the Log(N) - Log(L) curves corresponding to the differential box-counting approach. The almost perfect linearity of this curve indicates that a fractal approach seems to be valid for quantifying the observed differences. Similar curves (not shown) were obtained with the other techniques (e.g., power spectrum or blanket).

The fractal dimensions estimated from the two images with the box-counting technique are 2.53 and 2.39, respectively. It must be stressed that values obtained by other techniques are not identical (2.39 and 2.27, respectively, by the power spectrum approach, for instance). This discrepancy comes from the fact that all the techniques do not measure the same "fractal dimension." However, it is reinsuring to observe that all the estimations give a higher dimension for image 6a than for image 6b. Thus, even if estimating an absolute value of the "dimension" remains a difficult task, relative values (obtained with always the same method) can be used for ranking textured and fractal images.

On the basis of such calculations, we have undertaken studies related to the texture modifications observed in the following conditions: (1) cell pathology: during the different steps of interphase and of prophase of cancerous cells and (2) during the action of drugs leading to apoptosis of leukemic cells.

Quantification of the Chemical Content of a Specimen: the Example of Electron Energy Loss Imaging

Besides structural information, microscopists are also interested in the localization and quantification of the chemical species within the specimen. This can be done by microanalysis. Microanalytical techniques are very numerous and specialists in each of them have developed specific techniques for performing quantification from the type of data available. It is not possible to review all these methods within the framework of this article. Thus, we have chosen one single example to illustrate the potentialities and difficulties of performing such quantification. This example concerns transmission electron microscopy and, more specifically, the analysis of the energy lost by electrons when passing through a thin specimen. We have chosen this example because we think it is representative of the tendency which will concern most of the microanalytical techniques in the near future, i.e., the development of spectrum-imaging techniques. A spectrum-image is an image for which, at any pixel (x,y), a spectrum as a function of energy, I(E), or of wavelength, I(λ), is recorded. Such a data set can be processed along lines pertaining to spectroscopy (each spectrum $I_{x,y}(E)$ is processed independently), to image processing (each energy filtered image $I_E(x,y)$ is processed independently) or to mixed approaches which have still to be improved.

The spectrum-imaging technique is still in its infancy (Jeanguillaume and Colliex, 1989; Balossier *et al.*, 1991; Hunt and Williams, 1991; Lavergne *et al.*, 1992, 1994; Körtje, 1994). In routine experiments, which can be performed either with a TEM equipped with an energy filter or with a STEM equipped with a spectrometer, series of a few energy filtered images are recorded in the vicinity of the characteristic energy loss of the element to be studied. It must be stressed that with this type of microanalysis, unlike X-ray microanalysis or SIMS for instance, one single image cannot provide a

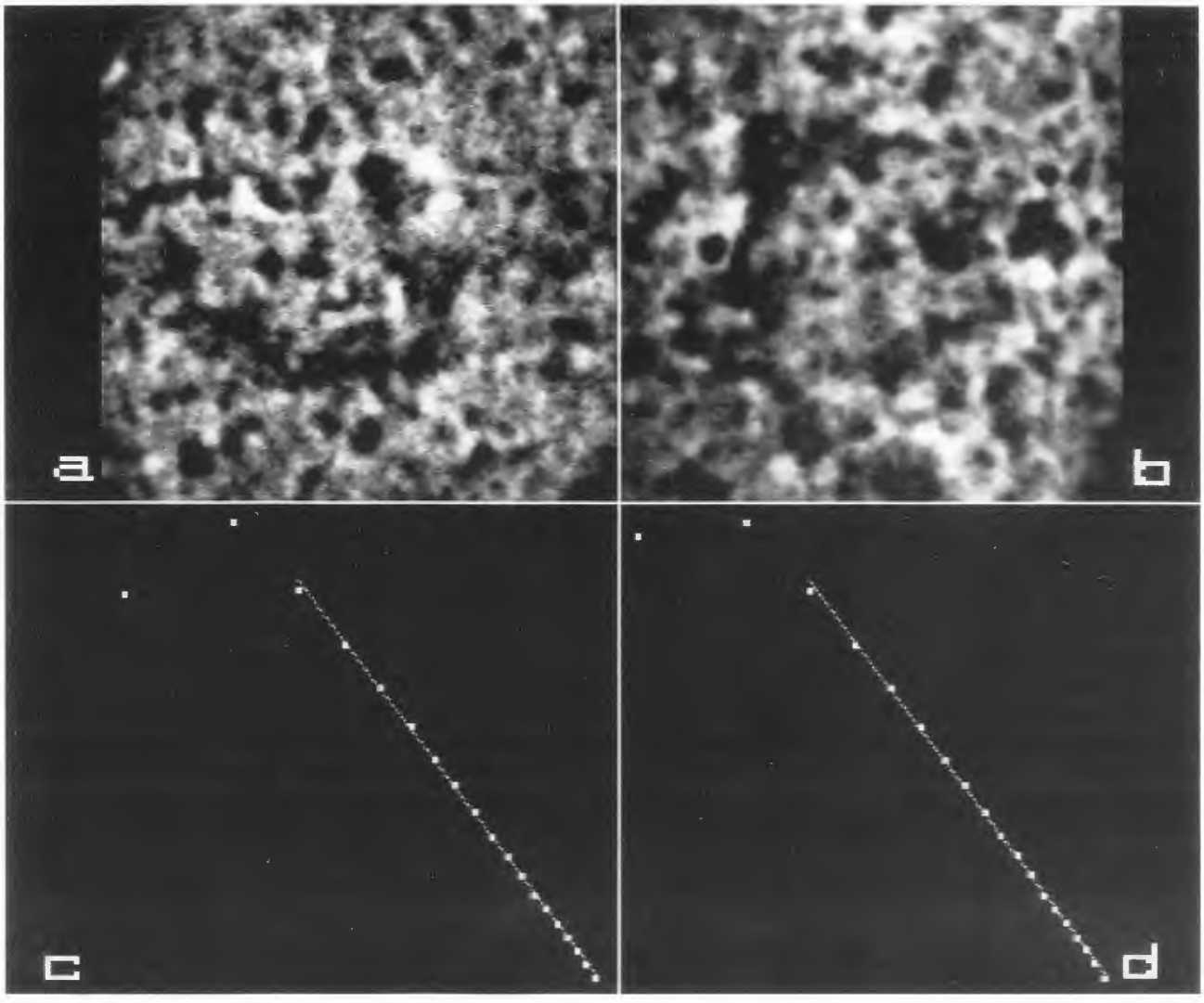

Figure 6. **(a and b)** Two examples of chromatin images obtained from cells in interphase (confocal microscopy). **(c and d)** Estimation of the fractal dimension by the box-counting method. Points represent the number of boxes necessary to cover the object (vertical: logarithmic scale) as a function of the box size (horizontal: logarithmic scale). The absolute value of the line slope gives the estimation of the fractal dimension (2.53 and 2.39 in these specific cases).

---

map of the concentration distribution, because the characteristic signal is always superimposed on an important background signal, which is not characteristic of the element under study. Thus, additional images must be recorded for energy losses below or far above the characteristic energy loss (Jeanguillaume *et al.*, 1978; Colliex, 1986; Leapman, 1986; Shuman *et al.*, 1986).

The question we wish to address in this section concerns the ways of extracting useful information (i.e., the "true" map of the elemental distribution and the amount of element at each position) from the experimentally recorded image sequence.

There are two groups of methods, each with some variants (Bonnet, 1995b). The first group is inherited from spectroscopic techniques. It consists in modelling the change in signal intensity as a function of the energy loss, for energy losses outside the characteristic region. The model obtained for the background can then be extrapolated inside the range of energy losses for which there is a characteristic signal. This extrapolated background is then subtracted from the experimental intensity values within this range, giving estimates of the desired net values of the characteristic signal. Finally, a comparison of the net intensity with the inelastic cross-sections provides an estimate of the numbers of atoms of the chemical element within the specimen column corresponding to the pixel studied. Repeating the procedure for all the pixels of the image sequence allows us to

build a 2D map of the number of atoms in the specimen columns. This procedure was first suggested by Jeanguillaume *et al.* (1978) and then extended by others. The model used was always the $A.E^{-R}$ curve proposed by Egerton (1986), where A and R are parameters to be established, and E is the energy loss. Several improvements were suggested by Bonnet *et al.* (1988), including: (1) the choice between different models, (2) a check of the consistency of the model ("ghost" image method), (3) the possibility of applying a semi-local model instead of a purely local (pixel level) or a purely global (image level) approach, and (4) the possibility of building statistically significant maps by performing a statistical analysis of the modelling process.

These developments in the context of STEM EELS were subsequently extended to Electron Spectroscopic Imaging (ESI) by Beckers *et al.* (1994).

Although this first approach is the most frequently used and has attained a high degree of sophistication (Leapman *et al.*, 1993; Colliex *et al.*, 1994; Leapman and Hunt, 1995), it is not completely satisfactory, for the following reasons: (1) It is mainly a local method: this means that, when processing a pixel data set, the content of the other pixels is completely disregarded. This makes the procedure statistically inefficient and thus noise sensitive. (2) As with any modelling approach, it is necessary to provide a model at the very beginning of the procedure. Thus, the question of the robustness of the quantitative results as a function of the choice of the model has to be considered.

For these two reasons, we have attempted to apply alternative methods to the processing of such image sequences (Hannequin and Bonnet, 1988; Bonnet and Hannequin, 1989). These methods, which belong to Multivariate Statistical Analysis (MSA), analyse the whole data set (i.e., all the pixels) at once and extract the pertinent information while discarding the redundant information. Their purpose is also to avoid the need for a mathematical model, at least during the first steps of the analysis. After our preliminary work, four variants of the approach have been suggested. We give only here a brief review of these variants.

[1] In the variant described by Trebbia and Bonnet (1990), the purpose of MSA is not to provide quantitative results directly. It is mainly to analyse qualitatively the data set (number of useful factors), to check its consistency (i.e., to detect possible experimental artefacts) and to eliminate a large part of the noise from it. For this last purpose, the data set (i.e., the energy-filtered image series) is reconstituted with only those factorial images that are believed to contain useful information (i.e., information related to the chemical content of the specimen). The other factorial images (related to noise or experimental artefacts) are discarded. Then, the reconstituted image series is processed along the "conventional" line (modelling, extrapolation of the background and background subtraction). Applications of this variant can be found in Trebbia and Mory (1990).

[2] The variant described by Hannequin and Bonnet (1988) contains the first attempt to obtain directly quantitative results from a MSA approach. For this purpose, the simple decomposition of the original data set into orthogonal components (which can be performed by Principal Components Analysis, Karhunen-Loeve Analysis or Correspondence Analysis) is not sufficient, because there is no reason why the characteristic signal should be orthogonal to the background. Thus, it is necessary to perform a second step, which consists in rotating the factorial axes so that each new axis can be identified with one of the underlying sources of information (e.g., background, characteristic signal or thickness). This "oblique analysis" is well known in chemistry (Malinowski and Howery, 1980) and in nuclear medicine (Di Paola *et al.*, 1982). The rotated axis corresponding to the characteristic signal then makes it possible to obtain the desired information in a quantitative way.

In the two other variants, the background extrapolation is performed in the factorial space, instead of in the "real" space (i.e., the space of the experiment, with the energy loss, E, as a variable):

[3] In the variant described by Bonnet *et al.* (1992b), only the images outside the characteristic range (i.e., images of the background) are submitted to MSA. After MSA, each of these images is characterized by coordinates (scores) on the two or three factorial axes, i.e., by a vector in a reduced (two or three-dimensional) factorial space. From these coordinates and the factorial images, the original image sequence can be reconstituted (see variant 1). The idea behind this variant is to reconstitute "fictitious" images instead of the real images. For this, we suggested keeping the factorial images as such and using "fictitious" weights (i.e., fictitious image scores on the factorial axes). These scores are of course not chosen at random but extrapolated from the coordinates of the real images (see Fig. 8 in Bonnet and Trebbia, 1992). The hypotheses implied by this procedure are the following:

(i) The fictitious images (which correspond to the background signal hidden by the characteristic signal) are sufficiently coherent with the experimental background images that they share the same factorial images.

(ii) The continuity between the real background images is sufficiently high that the unknown image scores can be extrapolated from the known ones according to a simple mathematical model (a polynomial of order one or two, for instance).

These hypotheses are assumed to be reasonable (see Bonnet *et al.*, 1992b) for a comparison of results

obtained by this variant and the conventional modelling approach).

[4] A fourth variant was suggested by Gelsema *et al.* (1994). The aim, as in the previous one, is to estimate the unknown background (at characteristic energy losses) from values of the background at non-characteristic energy losses. This is done following a different procedure: first, apply MSA to the whole image sequence. Then select the factorial axis which mostly represents the characteristic signal. Then, segment the corresponding factorial image into pixels containing a characteristic signal (say type A-pixels) and background-only pixels (say type B-pixels). Now, apply MSA to the set of type B-pixels only. Finally, apply the reconstitution procedure to type A-pixels using the results obtained after the analysis of type B-pixels. This allows us to obtain the background values for type A-pixels at energy losses above the characteristic edge. The remaining steps are trivial.

There is thus a wealth of suggestions for trying to overcome the limitations of the conventional modelling procedure. Unfortunately, there are not yet enough experimental results, especially in the field of biological applications with elements in small concentration, to draw a conclusion and to show whether one approach is superior to the others.

Finally, we would like to stress the fact that the discussion we have made concerning the processing of image series in electron energy loss microanalysis is not at all limited to this specific application. The duality modelling approach/MSA remains valid for many other types of imaging protocols. For instance, it is also pertinent in time-resolved fluorescence optical microscopy where videomicroscopic fluorescence imaging allows us to study ion (Ca^{2+} or Cl^{-} for instance) dynamics in cells (Bonnet and Zahm, 1995). It has also been employed in differential absorption X-ray imaging (Trebbia *et al.*, 1995).

Quantification Problems Related to Multi-Elemental Mapping

In the previous section, we have discussed the problems related to the extraction of quantitative information (i.e., the number of atoms of a given element contained in a column of the specimen) from a set of microanalytical images. Quantification in this context may also concern the area (in two dimensions) or the volume (in three dimensions, as in SIMS for instance) of the specimen with a given composition. When only one chemical element (or ion) is concerned, this kind of problem is closely related to the image segmentation problem encountered in structural image analysis, as discussed previously. Examples of such studies are given by De Bruijn *et al.* (1987) and Sorber *et al.* (1990, 1991), for instance.

With the improvement of microanalytical methods, we will be more and more often faced with the problem of multiple maps of a specimen, recorded either with the same technique or with complementary techniques (EELS and EDX, for instance). The first step of quantification, in this case, is to isolate regions of the specimen with homogeneous composition (segmentation step) on the basis of the different maps available. The second step consists in characterizing these different regions (size, shape, spatial organization and inter-relationships). We will only discuss the first step, since the other is not specific compared to structural two- or three-dimensional studies.

Concerning the segmentation of multivariate microanalytical maps, the only method which has been used extensively is the scatterplot approach (Jeanguillaume, 1985; Bright and Newbury, 1991; Kenny *et al.*, 1994). It is restricted to two maps (at most, three) of the same specimen and consists in building a two-dimensional histogram relating the content of one map to the content of the other one. In this plot, groups of pixels with homogeneous composition are displayed as clouds of points (clusters). One or several of these clouds can be selected interactively and back-mapped in the original image space.

This tool is noticeably inadequate if more than two or three maps are available or if an automation of the quantification procedure is expected. Recently, we have proposed several extensions to this procedure in order to handle a larger number of maps in a more or less automatic fashion:

[1] Extension of the scatterplot approach to a number N of maps greater than two or three:

With the conventional scatterplot approach, we can only deal with two data sets. If we choose for these two data sets two images of the experimental image series, we lose the information contained in the (N - 2) remaining ones and the scatterplot is of very limited usefulness. The idea (developed in Bonnet *et al.*, 1995) is to first build two data sets (synthetic images) which concentrate the whole information, and then to build a scatterplot with these two synthetic images. The problem is that there is an infinity of possible synthetic images. We have explored two variants: in the former one, we define "observers" of the N-dimensional data set (situated, for instance, at the corners of the hypercube) and the information coded is the distance of the different pixels (represented by points in the N-dimensional space, according to their intensity contents) to these observers. By combining the information "seen" by two such observers, we can build scatterplots which contain information related to the whole N-dimensional data set. In the second variant we have explored, the "observers" are no longer

points, but lines (in fact, diagonals of the hypercube).

The problem is still that there are several possibilities (pairs of corners, pairs of diagonals), some of them useful (i.e., clusters are displayed in the scatterplot when there are clusters in the data set) and some of them less useful. Thus, up to now, we have to select "good" scatterplots according to some fore-knowledge of the data set (separability of clusters). The problem of automatically mapping an N-dimensional data set onto a 2-dimensional space, with as little distortion as possible, has received attention for a long time in the field of pattern recognition (Sammon, 1969; Gelsema and Eden, 1980). We are currently investigating the possible application of these methods to multiple maps, and how they compare to neural networks (e.g., self-organizing maps, see Kohonen, 1988).

[2] Automatic handling of multiple maps without using the scatterplot approach:

The scatterplot approach is useful mainly if we want to have a visualization of the number of clusters, of their shape and of their relationships, or if we want to select one or several of them interactively. If we want to segment the N-dimensional data set automatically, this visualization is not absolutely necessary (although it can also be useful for checking the results). Thus, we have also suggested and experimented with two methods for the automatic handling of multiple microanalytical maps (Bonnet, 1995a). These two methods are:

(i) Clustering: numerous methods have been studied extensively in the field of data processing for clustering multi-dimensional data (Duda and Hart, 1973). Among them, the K-means and fuzzy C-means approaches can be used, together with criteria for estimating the number of homogeneous classes present in the data set. Work has still to be done for evaluating the influence of different parameters (especially, the choice of a distance function) on the quality of partitions obtained in practical situations.

(ii) Multivariate region growing: in the field of conventional image processing, region growing (also called "merge") is one of the methods of image segmentation (Horowitz and Pavlidis, 1976; Chen *et al.*, 1991). The extension of this approach to multi-dimensional data is straightforward and allows us to perform multi-image segmentation taking into account the spatial coordinates, at least in favorable situations.

[3] Multivariate Statistical Analysis:

The aim of the scatterplot approach is to display the correlation (or anti-correlation) between the intensities in two images, for different groups of pixels. It is also the aim of MSA, when more than two images are involved. Thus, multiple maps of a specimen can also be analysed by this technique. The different results which can be obtained are:

(i) the number of significant factors, which provides information about the number of independent "sources of information" present in the data set {see Bonnet *et al.* (1992b) and Bonnet and Trebbia (1992) for an in-depth discussion of this topic},

(ii) the correlation and anti-correlation between the different maps (scores of the different maps onto the significant factorial axes), and

(iii) the spatial distribution of the different sources of information (factorial images).

Detailed applications of this technique to series of X-ray spectra and of X-ray maps of liver cell nuclei cryo-prepared or prepared according to the potassium pyroantimonate method are described in Quintana and Bonnet (1994a,b).

Here again, it must be stressed that the problems discussed here are not limited to electron, ion or X-ray microanalysis, but are very general problems. The study of the co-localization of different fluorochromes in confocal microscopy, for example, is being very actively studied (e.g., Humbert *et al.*, 1992; Wansink *et al.*, 1994) and is clearly very similar to the quantification of multiple elemental maps.

Conclusion

In this paper, we have selected a few topics related to the general problem of quantification in imaging of biological specimens. Although we do not pretend to have covered the whole subject, we hope the examples we have chosen are representative of the state of the art in different domains of application of imaging: structural imaging, functional imaging and chemical imaging.

Concerning the first kind of images, we think that one of the most important tendencies is the advance from 2D quantification to 3D quantification. The efforts which have been made to extract quantitative information from 2D images can now be transposed to 3D digital data sets, provided these data sets are made free of the artefacts due to the anisotropy of the impulse response of imaging instruments. We have also noticed that, besides the quantification of lengths, surfaces, volumes, spatial distribution, etc., there is also a growing interest in the quantification of the textural appearance of biological structures.

Chemical imaging is also a domain in which instrumental improvements yield very sophisticated data sets, containing a wealth of information, which has to be decoded by no less sophisticated methods. We have shown that several approaches are presently in competition, but could also be used jointly in the near future. Essentially, the modelling approach can be used safely when an underlying model can be ascertained. Alternatively, Multivariate Statistical Analysis can be used to check the

consistency of the data set or as a preliminary step to analyse the content of a data set.

Since more and more multivariate data sets will be produced, there is also a need to introduce tools developed within the framework of multivariate pattern recognition as practical software for microscopists.

Finally, as a general conclusion, we would like to say that despite the many developments made during the last years, there is still much to be done before all the information recorded within images can be extracted. As the dimensionality of the recorded images increases (from two-dimensional images to three-dimensional ones, from mono-spectral to multi-spectral, from static to dynamic, from mono-modality to multi-modalities, etc.), the human visual system is less and less able to cope, and new computer algorithms will have to be developed to take over its role.

Acknowledgements

One of us (LL) is the recipient of a fellowship sponsored by the company BIORAD-France. Part of this work also benefitted from financial support from the "Association de Recherche contre le Cancer" (ARC). We would also like to express our thanks to F. Dolidon and B. Diallo for their help in programming some of the routines used for evaluating the fractal dimension.

References

Agard DA, Hiraoka Y, Shaw P, Sedat JW (1989) Fluorescence microscopy in three-dimensions. Meth Cell Biol **30**: 353-377.

Aguilar M, Anguiano E, Pancorbo M (1993) Fractal characterization by frequency analysis. II. A new method. J Microsc **172**: 233-238.

Anguiano E, Pancorbo M, Vasquez F, Aguilar M (1993) Fractal characterization by frequency analysis. I. Surfaces. J Microsc **172**: 223-232.

Balossier G, Thomas X, Michel J, Wagner D, Bonhomme P, Puchelle E, Ploton D, Bonhomme A, Pinon JM (1991) Parallel EELS elemental mapping in scanning transmission electron microscopy: Use of the difference methods. Microsc Microanal Microstruct **2**: 531-546.

Beckers ALD, de Bruijn WC, Gelsema ES, Cleton-Soeteman MI, Van Eijk HG (1994) Quantitative electron spectroscopic imaging in bio-medicine: Methods for image acquisition, correction and analysis. J Microsc **174**: 171-182.

Beghdadi A, Le Negrate A (1989) Contrast enhancement technique based on local detection of edges. CVGIP (Computer Vision, Graphics and Image Processing) **46**: 162-174.

Bertin E, Marcelpoil R, Chassery JM (1992) Morphological algorithms based on Voronoi and Delaunay graphs: Microscopic and medical applications. In: Image Algebra and Morphological Image Processing. Vol. III. SPIE, Bellingham, WA. pp. 356-357.

Bertin E, Parazza F, Chassery JM (1993) Segmentation and measurement based on 3D Voronoi diagram: Application to confocal microscopy. Comput Med Imag Graph **17**: 175-182.

Block A, von Bloh W, Klenke T, Schellnhuber HJ (1991) Multifractal analysis of the microdistribution of elements in sedimentary structures using images from scanning electron microscopy and energy dispersive X ray spectrometry. J Geophys Res **96**: 223-230.

Bonnet N (1995a) Preliminary investigation of two methods for the automatic handling of multivariate maps in microanalysis. Ultramicroscopy **57**: 17-27.

Bonnet N (1995b) Processing of images and image series: A tutorial review for chemical microanalysis. Mikrochim Acta **120**: 195-210.

Bonnet N (1995c) Speed increase in the deconvolution of multi-dimensional images. Internal Report INSERM U314 (available from authors).

Bonnet N, Hannequin P (1989) Chemical mapping and multivariate statistical analysis (prospect). Ultramicroscopy **28**: 248-251.

Bonnet N, Trebbia P (1992) Multi-dimensional data analysis and processing in electron-induced microanalysis. Scanning Microsc Suppl **6**: 163-177.

Bonnet N, Zahm JM (1995) Analysis of image sequences in fluorescence microscopy (non-moving objects). Internal report INSERM U314 (available from authors).

Bonnet N, Colliex C, Mory C, Tence M (1988) Developments in processing image sequences for elemental mapping. Scanning Microsc Suppl **2**: 351-364.

Bonnet N, Lucas L, Vautrot P, Gilbert N, Ploton D (1992a) Adaptive 3D image processing in confocal microscopy. Proc. 14th Int. Conf. IEEE Eng. Med. Biol. Soc. (abstract, copy available from N. Bonnet).

Bonnet N, Simova E, Lebonvallet, Kaplan H (1992b) New applications of multivariate statistical analysis in spectroscopy and microscopy. Ultramicroscopy **40**: 1-11.

Bonnet N, Dolidon F, Diallo B, Durand C, Herbin M (1994) A comparative study of algorithms for evaluating the fractal character of microscopic textures and surfaces. In: Proceedings of the 13th International Conference of Electron Microscopy. Editions de Physique, Les Ulis, France. pp. 445-446 (abstract).

Bonnet N, Herbin M, Vautrot P (1995) Extension of the scatterplot approach to multiple images. Ultramicroscopy **60**: 349-355.

Bright DS, Newbury DE (1991) Concentration histogram imaging. Anal Chem **63**: 243A-250A.

Brugal G (1984) Image analysis of microscopic preparations. Meth Achiev Exp Pathol **11**: 1-33.

Castelman KR (1979) Digital Image Processing. Prentice Hall, Englewood Cliffs.

Chaudhuri BB, Sarkar N, Kundu P (1993) Improved fractal geometry based texture segmentation technique. IEE Proc E **140**: 233-241.

Chen SY, Lin WC, Chen CT (1991) Split-and-merge image segmentation based on localized feature analysis and statistical tests. CVGIP: Graphical Models Image Process **53**: 457-475.

Colliex C (1986) Electron energy-loss spectroscopy analysis and imaging of biological specimens. Annals NY Acad Sci **483**: 311-325.

Colliex C, Tencé M, Lefèvre E, Mory C, Gu H, Bouchet D, Jeanguillaume C (1994) Electron energy loss spectrometry mapping. Mikrochim Acta **114/115**: 71-87.

Cross SS (1994) The application of fractal geometric analysis to microscopic images. Micron **25**: 101-113.

De Bruijn WC, Koerten HK, Cleton-Soeteman, Blok-van Hoek CJG (1987) Image analysis and X-ray microanalysis in cytochemistry. Scanning Microsc **1**: 1651-1667.

Di Paola R, Bazin JP, Aubry F, Aurengo A, Cavailloles F, Herry JY, Kahn E (1982) Handling of dynamic sequences in nuclear medicine. IEEE Trans Nucl Sci **NS29**: 1310-1321.

Duda RO, Hart PE (1973) Pattern Classification and Scene Analysis. Wiley Interscience, New York. pp. 189-256.

Egerton RF (1986) Electron Energy-Loss Spectroscopy in the Electron Microscope. Plenum Press, New York. pp. 229-287.

Fernandez E, Eldred WD, Ammermüller J, Block A, von Bloh W, Kolb H (1994) Complexity and scaling properties of amacrine, ganglion, horizontal and bipolar cells in the turtle retina. J Compar Neurol **347**: 397-408.

Frank J (ed.) (1992) Electron Tomography. Three-Dimensional Imaging with the Transmission Electron Microscope. Plenum Press, New York.

Galloway MM (1975) Texture analysis using gray level run lengths. CGIP (Computer Graphics and Image Processing) **4**: 172-179.

Gangepain JJ, Roques-Carmes C (1986) Fractal approach to the two dimensional and three dimensional surface roughness. Wear **109**: 119-126.

Gelsema ES, Eden G (1980) Mapping algorithms in ISPAHAN. Patt Rec **12**: 127-136.

Gelsema ES, Beckers ALD, de Bruijn WC (1994) Optimal conditions for the use of correspondence analysis for element determination in EELS images. J Microsc **174**: 161-169.

Gilbert N, Lucas L, Klein C, Menager M, Bonnet N, Ploton D (1995) Three-dimensional co-location of RNA polymerase I and DNA during interphase and mitosis by confocal microscopy. J Cell Science **108**: 115-125.

Gratin C, Meyer F (1992) Morphological three-dimensional analysis. Scanning Microsc Suppl **6**: 129-135.

Guilak F (1994) Volume and surface area measurement of viable chondrocytes *in situ* using geometric modelling of serial confocal sections. J Microsc **173**: 245-256.

Hannequin P, Bonnet N (1988) Application of multivariate statistical analysis to energetic image series. Optik **81**: 6-11.

Haralick RM (1979) Statistical and structural approaches to texture. Proc IEEE **67**: 786-804.

Hawkes PW (ed.) (1980) Computer Processing of Electron Microscope Images. Springer-Verlag, Berlin, Germany.

Höfers C, Baumann P, Hummer G, Jovin TM, Arndt-Jovin DJ (1993) The localization of chromosome domains in human interphase nuclei. Three-dimensional distance determinations of fluorescence in-situ hybridization signals from confocal laser scanning microscopy. Bioimaging **1**: 96-106.

Holmes TJ, Liu Y (1989) Richardson-Lucy/maximum-likelihood image restoration algorithm for fluorescence microscopy: Further testing. Appl Opt **28**: 4930-4938.

Holmes TJ, Liu Y, Khosla D, Agard DA (1991) Increased depth of field and stereo pairs of fluorescence micrographs via inverse filtering and maximum-likelihood estimation. J Microsc **164**: 217-237.

Horowitz SL, Pavlidis T (1976) Picture segmentation by a tree transversal algorithm. J Assoc Comput Mach **23**: 368-388.

Humbert C, Santisteban, Usson MS, Robert-Nicoud M (1992) Intranuclear co-location of newly replicated DNA and PCDNA by simultaneous immunofluorescent labelling and confocal microscopy in MCF-7 cells. J Cell Sci **103**: 97-103.

Hunt JA, Williams DB (1991) Electron energy-loss spectrum-imaging. Ultramicroscopy **38**: 47-73.

Jain AK, Farrokhnia F (1991) Unsupervised texture segmentation using Gabor filters. Patt Rec **24**: 1167-1186.

Jansson PA, Hunt RH, Plyler EK (1970) Resolution enhancement of spectra. J Opt Soc Am **60**: 596-599.

Jeanguillaume C (1985) Multi-parameter statistical analysis of STEM micrographs. J Microsc Spectrosc Electron **10**: 409-415.

Jeanguillaume C, Colliex C (1989) Spectrum-image: The next step in EELS digital acquisition and processing. Ultramicroscopy **28**: 252-257.

Jeanguillaume C, Trebbia P, Colliex C (1978) About the use of electron energy loss spectroscopy for

chemical mapping of thin foils with high spatial resolution. Ultramicroscopy **3**: 138-142.

Jeulin D (1988) Mathematical morphology and materials image analysis. Scanning Microsc Suppl **2**: 165-183.

Jin XC, Ong SH, Jayasooriah (1995) A practical method for estimating fractal dimension. Patt Rec Lett **16**: 457-464.

Katsaggelos AK (ed.) (1991) Digital Image Restoration. Springer-Verlag, Berlin. pp. 1-20.

Kawata S, Ichioka Y (1980) Iterative image -restoration of linearly degraded images. II. Reblurring procedure. J Opt Soc Am **70**: 768-772.

Keller JM, Chen S, Crownover RM (1989) Texture description and segmentation through fractal geometry. CVGIP **45**: 150-166.

Kenny PG, Barkshire IR, Prutton M (1994) Three-dimensional scatter diagrams: Application to surface analytical microscopy. Ultramicroscopy **56**: 289-301.

Keough KMV, Hyam P, Pink DA, Quinn B (1991) Cell surfaces and fractal dimensions. J Microsc **163**: 95-99.

Kett P, Geiger B, Ehemann V, Komitowski D (1992) Three-dimensional analysis of cell structures visualized by confocal scanning laser microscopy. J Microsc **167**: 169-179.

Kohonen T (1988) Self-Organization and Associative Memory. Springer-Verlag, Berlin. pp. 119-184.

Komitowski D, Zinser G (1985) Quantitative description of chromatin structure during neoplasia by the method of image processing. Anal Quantit Cytol Histol **7**: 178-182.

König D, Carvajal-Gonzalez S, Downs AM, Vassy J, Rigaut JP (1991) Modelling and analysis of 3D arrangements of particles by point processes with examples of application to biological data obtained by confocal scanning laser microscopy. J Microsc **161**: 405-433.

Körtje KH (1994) Image-EELS: Simultaneous recording of multiple electron energy-loss spectra from series of electron spectroscopic images. J Microsc **174**: 149-159.

Landeweerd GH, Gelsema ES (1978) The use of nuclear texture parameters in the automatic analysis of leukocytes. Patt Rec **10**: 57-61.

Lavergne JL, Martin JM, Belin M (1992) Interactive electron energy-loss elemental mapping by the "imaging-spectrum" method. Microsc Microanal Microstruct **3**: 517-528.

Lavergne JL, Foa C, Bongrand P, Seux D, Martin JM (1994) Application of recording and processing of energy-filtered image sequences for the elemental mapping of biological specimens: Imaging-spectrum. J Microsc **174**: 195-206.

Leapman RD (1986) Scanning transmission electron microscope (STEM) elemental mapping by electron energy-loss spectroscopy. Annals NY Acad Sci **483**: 326-338.

Leapman RD, Hunt JA (1995) Compositional imaging with electron energy loss spectroscopy. J Microsc Soc Am **1**: 93-108.

Leapman RD, Hunt JA, Buchanan RA, Andrews SB (1993) Measurement of low calcium concentrations in cryosectioned cells by parallel-EELS mapping. Ultramicroscopy **49**: 225-234.

Lipkin BS, Lipkin LE (1974) Textural parameters related to nuclear maturation in the granulocytic leukocytic series. J Histochem Cytochem **22**: 583-593.

Lorensen WE, Cline HE (1987) Marching cubes: High resolution 3D surface reconstruction algorithm. Comput Graph **21**: 163-169.

Lucas L (1995) Reconstruction, Visualisation et Quantification Tridimensionnelle: Application à la Microscopie Confocale (Three-dimensional Reconstruction, Visualization and Quantification: Application to Confocal Microscopy). Doctoral Thesis. University of Reims, France.

Lucas L, Gilbert N, Ploton D, Bonnet N (1996a) Visualization of volume data in confocal microscopy: comparison and improvements of volume rendering methods. J Microsc **181**: 238-252.

Lucas L, Trunde F, Bonnet N (1996b) Time-dependent 3D data set rendering: An extension of the morphing technique. J Visual Comput Anim, in press.

Lucy LB (1974) An iterative technique for the rectification of observed distributions. Astron J **79**: 745-765.

Malinowski E, Howery D (1980) Factor Analysis in Chemistry. Wiley-Interscience, New York. pp. 23-58.

Mandelbrot BB (1982) The Fractal Geometry of Nature. Freeman, San-Francisco.

Maragos P (1994) Fractal signal analysis using mathematical morphology. Adv Electron Electron Phys **88**: 199-246.

Maragos P, Schafer RW (1990) Morphological systems for multidimensional signal processing. Proc IEEE **78**: 690-710.

Meyer F (1992) Mathematical morphology: From two dimensions to three dimensions. J Microsc **165**: 5-28.

Monck JR, Oberhauser AF, Keating TJ, Fernandez JM (1992) Thin-section ratiometric Ca^{2+} images obtained by optical sectioning of Fura-2 loaded mast cells. J Cell Biol **116**: 745-759.

Nonnenmacher TF (1994) Spatial and temporal fractal patterns in cell and molecular biology. In: Fractals in Biology and Medicine. Nonnenmacher TF, Losa GA, Weibel ER (eds.). Birkhauser Verlag, Basel, Switzerland. pp. 22-37.

Nonnenmacher TF, Baumann G, Barth A, Losa GA

(1994) Digital image analysis of self-similar cell profiles. Int J Biomed Comput **37**: 131-138.

Parazza F, Bertin E, Wozniak Z, Usson Y (1995) Analysis of the spatial distribution of AgNOR proteins in cell nuclei using simultaneous confocal scanning laser fluorescence and transmitted light microscopy. J Microsc **178**: 251-260.

Pawley JB (ed.) (1990) Handbook of Biological Confocal Microscopy. Plenum Press. New York.

Peleg S, Naor J, Hartley R, Avnir D (1984) Multiple resolution texture analysis and classification. IEEE Trans PAMI (Pattern Analysis and Machine Intelligence) **6**: 518-523.

Pentland AP (1984) Fractal-based description of natural scenes. IEEE Trans PAMI **6**: 661-674.

Ploton D, Gilbert N, Menager M, Kaplan H, Adnet JJ (1994) Three-dimensional co-location of nucleolar argyrophilic components and DNA in cell nuclei by confocal microscopy. J Histochem Cytochem **42**: 137-148.

Pratt WK, Faugeras O, Gagalowicz A (1981) Applications of stochastic texture field models to image processing. Proc IEEE **69**: 542-551.

Pressman NJ (1976) Markovian analysis of cervical cell images. J Histochem Cytochem **24**: 138-144.

Preston K (1991) Three-dimensional mathematical morphology. Image Vision Comput **9**: 285-295.

Prokop RJ, Reeves AP (1992) A survey of moment-based techniques for unoccluded object representation and recognition. CVGIP: Graph Mod Im Proc **54**: 438-460.

Quintana C, Bonnet N (1994a) Multivariate statistical analysis (MSA) applied to X-ray spectra and X-ray mapping of liver cell nuclei. Scanning Microsc **8**: 563-586.

Quintana C, Bonnet N (1994b) Improvements of biological X-ray microanalysis: Cryoembedding for specimen preparation and multivariate statistical analysis for data interpretation. Scanning Microsc Suppl **8**: 83-99.

Richardson WH (1972) Bayesian-based iterative method of image restoration. J Opt Soc Am **62**: 55-59.

Rigaut JP (1988) Automated image segmentation by mathematical morphology and fractal geometry. J Microsc **150**: 21-30.

Rigaut JP, Vassy J, Herlin P, Duigou F, Masson E, Briane D, Foucrier J, Carvajal-Gonzalez S, Downs A, Mandard AM (1991) Three-dimensional DNA image cytometry by confocal scanning laser microscopy in thick tissue blocks. Cytometry **12**: 511-524.

Russ JC (1990a) Computer-Assisted Microscopy. Plenum Press, New-York.

Russ JC (1990b) Processing images with a local Hurst operator to reveal textural differences. J Comp Ass Microsc **2**: 249-257.

Sammon JW (1969) A nonlinear mapping for data structure analysis. IEEE Trans Comp **C-18**: 401-409.

Shuman H, Chang CF, Buhle EL, Somlyo AP (1986) Electron energy-loss spectroscopy: Quantitation and imaging. Annals NY Acad Sci **483**: 295-310.

Smeulders AW, Leyte-Veldstra L, Ploem JS, Cornelisse CJ (1979) Texture analysis of cervical cell nuclei by segmentation of chromatin patterns. J Histochem Cytochem **27**: 199-203.

Sorber CWJ, Van Doort JB, Ringeling PC, Cleton-Soteman MI, de Bruijn WC (1990) Quantitative energy-filtered image analysis in cytochemistry. II. Morphometric analysis of element-distribution images. Ultramicroscopy **32**: 69-79.

Sorber CWJ, Ketelaars GAM, Gelsema ES, Jongkind JF, de Bruijn WC (1991) Quantitative analysis of electron energy-loss spectra from ultrathin-sectioned biological material. I. The application of Bio-standards for quantitative analysis. J Microsc **162**: 43-54.

Trebbia P, Bonnet N (1990) EELS elemental mapping with unconventional methods. I. Theoretical basis: Image analysis with multivariate statistics and entropy concepts. Ultramicroscopy **34**: 165-178.

Trebbia P, Mory C (1990) EELS elemental mapping with unconventional methods. II. Applications to biological specimens. Ultramicroscopy **34**: 179-203.

Trebbia P, Wulveryck JM, Bonnet N (1995) Progress in quantitative mapping by X-ray imaging. Microbeam Analysis **4**: 85-104.

Turner JN (ed.) (1981) Three-dimensional Ultrastructure in Biology. Methods in Cell Biology. Vol. 22. Academic Press. New York.

Unser M, Eden M (1989) Multiresolution feature extraction and selection for texture segmentation. IEEE Trans PAMI **11**: 717-728.

Usson Y, Parazza F, Jouk PS, Michalowicz G (1994) Method for the study of the three-dimensional orientation of the nuclei of myocardial cells in fetal human heart by means of confocal scanning laser microscopy. J Microsc **174**: 101-110.

Vautrot P, Bonnet N (1994) Evaluation of different local processing algorithms for the improvement of the signal-to-noise ratio. In: Proceedings of the 13th International Congress of Electron Microscopy. Editions de Physique, Les Ulis, France. pp. 429-430 (abstract).

Vautrot P, Bonnet N (1995) Application des ondelettes splines à la segmentation d'images texturées. Comparaison avec les filtres de Gabor (Application of spline wavelets to the segmentation of textured images. Comparison with Gabor filters). In: Proc 15th Colloque GRETSI (Groupement de Recherche En Traitement du Signal et des Images), Juan-les-Pins. Picinbono B (ed.). Zimmermann, Villeneuve-Loubet, France. pp. 597-600.

Visser TD, Oud JL, Brakenhoff GJ (1992) Refrac-

tive index and axial distance measurements in 3-D microscopy. Optik **90**: 17-19.

Wansink DG, Manders E, van der Kraan I, Aten JA, van Driel R, de Jong L (1994) RNA polymerase II transcription is concentrated outside replication domains throughout S-phase. J Cell Sci **107**: 1449-1456.

Willis B, Roysam B, Turner JN, Holmes TJ (1993) Iterative, constrained 3-D image reconstruction of transmitted light bright-field micrographs based on maximum likelihood estimation. J Microsc **169**: 347-361.

Young IT, Verbeek PW, Mayall H (1986) Characterization of chromatin distribution in cell nuclei. Cytometry **7**: 467-474.

Discussion with Reviewers

E.S. Gelsema: It is interesting to see that the two methods for the estimation of fractal dimensions rank the two images corresponding to two different states of interphase in the same way. This does not, however, show that different states of interphase can be discriminated in this way. It is true that the authors do not state that, but they seem to imply it. Do the authors have any evidence that a fractal dimension estimation method can be used for this more ambitious purpose?

Authors: It is true that we hope to be able to discriminate different states of interphase through the quantification of variations in the textural appearance of images. But, in the present state of our investigations, we do not claim that the fractal dimension is a parameter sufficient for this purpose. In fact, the fractal dimension variation between different images is rather weak and has to be compared to the biological variability before any conclusion can be drawn. Our limited set of experiments do not allow us to draw such a conclusion. Moreover, the fractal dimension is not the only parameter which can be estimated. The porosity, or different fractal signatures, or multi-fractal parameters, can also be used for characterizing the chromatin aspect. Which parameter is better suited for the purpose of chromatin image ranking in different situations is still subject to study. On the other hand, it is not proven that fractal parameters are better candidates than other textural features (based on Markov random fields, for instance) for this characterization.

E.S. Gelsema: As far as I am aware, while many clustering techniques have been proposed in the context of pattern recognition, the problem of determining the optimal number of clusters, given a data set is not solved by any of them. I would be interested in methods which can validate various clustering solutions with different numbers of clusters N, i.e., which operate on a clustering criterion which is valid for a range of values of N. In my opinion, this is a larger problem than choosing a particular distance function, the influence of which is rather well known.

Authors: We agree with your comment. The intrinsic dimensionality (i.e., the "true" number of classes) of a data set is a parameter which has to be evaluated during the course of clustering, and this is not an easy task. In parallel to the large number of clustering techniques which have been suggested, a large number of "objective" parameters have been proposed for evaluating the quality of a partition. The problem is that these "objective" criteria are not often self-consistent and generally produce different results for a given data set. The allowed space does not permit us to develop our answer as necessary {see Duda and Hart (1973) as a classical reference}. We just give some indications and additional references.

Within the framework of the K-means procedure, some criteria which can be used for estimating the "true" number of clusters are: (**1**) the position of an elbow (or turning point) of the within-cluster distance computed as a function of the number of clusters, (**2**) combinations of the within-class variance and of the between-class variance (Fukunaga, 1972), (**3**) local eigenvalues of the covariance matrix (Verveer and Duin, 1995) and (**4**) the minimum of the Akaike information criterion (AIC) (Akaike, 1974).

A comprehensive list of references, together with some new developments, is given by Carazo *et al.* (1990) for clustering within the framework of fuzzy logic.

It must be stressed that automatic classification procedures can only be envisaged in rather favorable situations, i.e., when the different clusters are reasonably separated. When the clusters are strongly overlapping, attempting to determine automatically the number of clusters and to perform classification on this basis can lead to very misleading conclusions.

N.K. Tovey: You mention the "quantification problems related to multi-elemental mapping" and in particular, the problem faced when there are more than two images present. Would you please comment on the approaches to solve this problem which have been in widespread use in Remote Sensing for many years but have been used relatively little in image analysis despite the similarity of the techniques. Papers already written adapting the remote sensing technique to image analysis are covered in Tovey *et al.* (1992a,b).

Authors: As written by one of the referees (J.A. Swift), we consider the work described in the papers you mention as "a most elegant piece of work." But we do not think that it can be compared to the (very preliminary) description we made of automatic classification. The main reason that these two approaches cannot be

compared is that your papers describe **supervised** multi-spectral classification while what we describe is **unsupervised** classification. For supervised classification, you need to delineate training areas composed of "pure" material (quartz, feldspar, etc.). As you write yourself, good classification results can only be obtained (whatever the classification of the procedure used) "provided that a correct selection of training area has been made" (Tovey *et al.*, 1992b, p. 273). We have no doubt that experts can designate valid training areas in the fields of remote sensing and of material science applications. Thus, many **supervised** procedures, including maximum likelihood classification, but also neural networks approaches, can be envisaged. In the field of biological applications, we think that reliable "prototypes" (training areas) are more difficult to obtain. This is the reason why we are exploring the way of **unsupervised** classification. We expect that if different classes of pixels (representing different composition of the specimen, or different co-localization of fluorescent markers) are present, they can be identified as different clusters in the multi-dimensional data space without the need to use a training set.

N.K. Tovey: How does the Jansson-van Cittert procedure for image reconstruction, which appear to be a non-linear iterative approach compare with the techniques described in several papers by Shaw and Razaz {e.g., Razaz *et al.* (1993)}?

Authors: As reported in the section of this review devoted to image restoration, a number of methods have been suggested for trying to cope with the limitations of the imaging instruments and especially the loss of axial resolution due to the depth of field. In agreement with several authors, we consider that, in general, non-linear algorithms perform better than linear ones, but the detailed comparison between various non-linear methods is difficult to perform. What we suggest is to simulate images (or volumes) as similar as possible to the experimental data to process, to simulate the degradation process and to check the ability of the different algorithms to restore the simulated image. We conducted such experiments with the algorithms we have described, but we cannot ascertain that the results we have obtained with our data sets can be generalized.

Additional References

Akaike H (1974) A new look at the statistical model identification. IEEE Trans Automat Control **AC-19**: 716-723.

Carazo JM, Rivera FF, Zapata EL, Radermacher M, Frank J (1990) Fuzzy set-based classification of electron microscopy images of biological macromolecules with an application to ribosomal particles. J Microsc **157**: 187-203.

Fukunaga K (1972) Introduction to Statistical Pattern Recognition. Academic Press, New York. pp. 508-562.

Razaz M, Lee R, Shaw P (1993) A nonlinear iterative least-squares algorithm for image restoration. Proc IEEE Nonlinear Signal Processing, 4.1-4.6.

Tovey NK, Krinsley DH, Dent DL, Corbett WM (1992a) Techniques to quantitatively study the microfabric of soils. Geoderma **53**: 217-235.

Tovey NK, Dent DL, Krinsley DH, Corbett WM (1992b) Processing multi-spectral SEM images for quantitative microfabric analysis. Scanning Microsc Suppl **6**: 269-282.

Verveer PJ, Duin PW (1995) An evaluation of intrinsic dimensionality estimators. IEEE Trans PAMI **17**: 81-86.